JOURNAL OF MATERIALS SCIENCE 24 (1989) 3824–3830

Preparation of silicon carbide powders by chemical vapour deposition of the SiH_4–CH_4–H_2 system

LIDONG CHEN, TAKASHI GOTO, TOSHIO HIRAI
Institute for Materials Research, Tohoku University, Sendai 980, Japan

Chemical vapour deposition (CVD) of the $SiH_4 + CH_4 + H_2$ system was applied to synthesize β-silicon carbide powders in the temperature range 1523 to 1673 K. The powders obtained at 1673 K were single-phase β-SiC containing neither free silicon nor free carbon. The powders obtained below 1623 K were composite powders containing free silicon. The carburization ratio (SiC/(SiC + Si)) increased with increasing reaction temperature and total gas flow rate, and with decreasing reactant concentration. The average particle sizes measured by TEM ranged from 46 to 114 nm. The particle size increased with the reaction temperature and gas concentration but decreased with gas flow rate. The β-SiC particles obtained below 1623 K consisted of a silicon core and a β-SiC shell, as opposed to the β-SiC particles obtained at 1673 K which were hollow. Infrared absorption peaks were observed at 940 and 810 cm^{-1} for particles containing a silicon core; whereas a single peak at about 830 cm^{-1} with a shoulder at about 930 cm^{-1} was observed for the β-SiC hollow particles. The lattice parameter of β-SiC having a carburization ratio lower than 70 wt%, was larger than that of bulk β-SiC and decreased with the increasing carburization ratio. However, when the carburization ratio exceeded 70 wt%, the lattice parameter became approximately equal to that of bulk β-SiC.

1. Introduction

High-density silicon carbide (SiC) sintered bodies are widely utilized for high-temperature structural and electronic materials. Furthermore, porous silicon carbide prepared by intentionally introducing pores in the sintered body shows good machinability [1], high thermal shock resistance and high efficiency for thermoelectric power [2]. These characteristics make it a promising new material. Several nano-composites, having dispersions of approximately nanometre size in the SiC matrix, have been synthesized [3]. Many attractive properties have been discovered in these composites [3]. An attempt has been made to increase the heat-insulation characteristics of SiC by introducing nanometre-size pores in the SiC body [4]. This material is also a nano-composite. Hollow SiC particles are a promising starting material in order to produce an SiC sintered body containing nano-pores. In the present study, the hollow β-SiC particles were prepared by chemical vapour deposition (CVD) using $SiH_4 + CH_4 + H_2$ as source gases. The effects of reaction conditions on the structures of the particles were investigated.

2. Experimental procedure

The vapour-phase reaction was carried out in a flow-type reactor at a total gas pressure (P_{tot}) of 0.1 MPa. The schematic diagram of the apparatus for synthesizing powders is shown in Fig. 1. The reaction chamber consisted of a reaction-sintered (RS) SiC tube placed within a mullite tube which was positioned in a resistance furnace. The reactant gases were introduced into the reaction chamber through stainless steel nozzles. The product powders were collected in a flask having a 65 mesh brass filter. CH_4 (99.99%) and H_2 (99.999%) gases along with a gas mixture of H_2 + 10.0 vol % SiH_4 (99.9999%) were used as source gases. Reaction temperatures ranged from 1523 to 1673 K. The preparation experiments were carried out at total gas flow rates (FR) of 1.8×10^{-5} and 2.7×10^{-5} m^3 sec^{-1} and at SiH_4 concentrations of 2 and 3.6 mol %. The $[SiH_4]/[CH_4]$ mole ratio was fixed at 0.5. The preparation conditions are summarized in Table I.

The shape and structure of resulting particles were observed by transmission electron microscopy (TEM) (JEOL: JEM-2000EX). The specific surface area was determined by three point BET method using a sorptograph (Shimadzu: ADS-1B). The powder density was measured by pycnometry using toluene. The infrared absorption spectra (IR) were obtained by the KBr pellet method using spectrophotometer (Japan Spectroscopic: IR-G) at wavenumbers from 400 to 4000 cm^{-1}. The crystal phases and the lattice parameter were determined by X-ray diffractometry (Rigaku: RAD-IIB, nickel-filtered CuKα). The SiC/(SiC + Si) content ratio, (carburization ratio, wt %) was estimated from the X-ray diffraction intensity of (1 1 1) peaks of β-SiC and silicon phases.

3. Results and discussion

3.1. Formation and composition of SiC particles

From the results of the X-ray diffraction analyses the powder obtained at 1673 K was identified as single-

0022–2461/89 $03.00 + .12

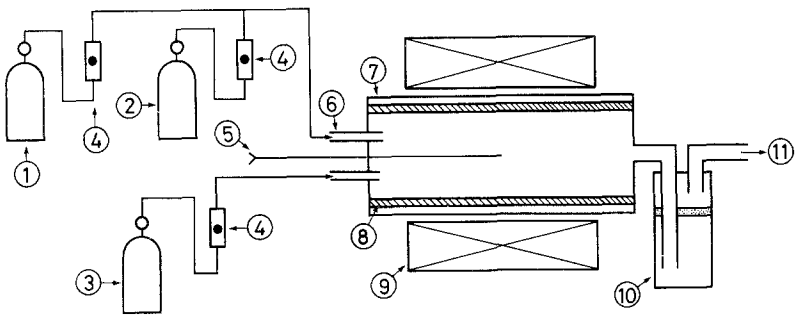

Figure 1 Schematic diagram of the apparatus for synthesizing SiC powder. (1) $SiH_4 + H_2$ mixture gas, (2) H_2 gas, (3) CH_4 gas, (4) flow meter, (5) thermocouple, (6) stainless steel nozzle, (7) mullite tube (internal diameter 35 mm), (8) RS-SiC tube (internal diameter 20 mm), (9) SiC resistance furnace, (10) collecting flask and filter, (11) gas outlet.

phase β-SiC. Both β-SiC and silicon-phases were present below 1623 K at each reactant concentration and gas flow rate. The SiC powder yield, calculated from the input of SiH_4 source, increased from 5 to 41% with the increase of reaction temperature and total gas flow rate. The powders of the single phase SiC, free of excess silicon, were grey in colour. The colour changed from grey to yellow to brown as the excess silicon content increased.

Fig. 2 shows the effect of the reaction temperature on the carburization ratio. From Fig. 2, at a constant concentration of SiH_4 and CH_4, the carburization ratio increases with the increase of reaction temperature and total gas flow rate; while at a constant gas flow rate, the carburization ratio increases with decrease of the SiH_4 and CH_4 reactant concentration. Table II summarizes the carburization ratio, SiC yield and colour of the powders.

Fig. 3 shows the CVD phase diagram for the SiH_4–CH_4–H_2 system calculated with the optimization method [5] using thermodynamic data at $[SiH_4] + [CH_4] = 6\,mol\,\%$, $FR = 2.7 \times 10^{-5}\,m^3\,sec^{-1}$ and $P_{tot} = 0.1$ MPa. Under equilibrium conditions, silicon and β-SiC phases form at a mole ratio of $[CH_4]/[SiH_4] < 1$ at any reaction temperature. When the ratio $[CH_4]/[SiH_4] > 1$, β-SiC phase containing excess carbon forms above 1100 K, and single-phase β-SiC forms below 1100 K. The preparation conditions for the present study are: $[CH_4]/[SiH_4] = 2$, reaction temperature from 1523 to 1673 K. Therefore, β-SiC + C phases are expected to form under equilibrium conditions. However, in the present experiment, powders containing silicon and β-SiC phases or single-phase β-SiC were obtained.

The formation of SiC particles from the SiH_4–CH_4–H_2 system is generally considered to be a two-step process [6]. At first, silicon particles are formed by the decomposition of SiH_4 gas and subsequently carburized into β-SiC by CH_4. Then silicon diffuses to the outer surface of the particle and reacts with CH_4 to form SiC. It was reported that SiH_4 was completely decomposed to silicon particles above 873 K [6]. The results of thermodynamical calculations shown in Fig. 3 were not in agreement with the present experiments. The reasons for this difference could be that the carburization process of silicon particles is very slow or that the formation of carbon particles by the decomposition of CH_4 in H_2 is kinetically difficult. Another possibility is that, because reactant gases are exposed to the high-temperature region in the furnace for 1 sec or less, the temperature of the reactant gases or that of the formed particles may be lower than the furnace temperature.

3.2. Shape and structure of particles

Figs 4a, b and c show the electron microscopic bright-field image, the β-SiC (1 1 1) dark-field image and the selected-area electron diffraction pattern, respectively, of the particles obtained at 1673 K. It is clearly seen that these particles are hollow β-SiC. Under all preparation conditions the β-SiC particles obtained are polycrystalline consisting of small β-SiC crystallites. The crystallite sizes measured from the micrographs agree with those measured by the broadening X-ray line of the β-SiC (1 1 1), (2 2 0) and (3 1 1) peaks that are shown in Table III.

Figs 5a, b and c show the bright-field image, the Si (1 1 1) dark-field image and the selected-area electron

TABLE I Preparation conditions of powders

Run no.	Reaction temperature (K)	Total gas flow rate (FR) ($m^3\,sec^{-1}$)	Reactant concentration (mol %)	
			$[SiH_4]$	$[CH_4]$
A125	1523	1.8×10^{-5}	3.6	7.2
A130	1573			
A135	1623			
A140	1673			
B125	1523	2.7×10^{-5}	3.6	7.2
B130	1573			
B135	1623			
B140	1673			
C125	1523	2.7×10^{-5}	2.0	4.0
C130	1573			
C135	1623			
C140	1673			

TABLE II Carburization ratio, SiC yield and colour of powders

Run no.	Carburization ratio SiC/(SiC + Si) (wt %)	SiC yield (%)	Colour
A125	16	5	brown-yellow
A130	27	6	yellow
A135	45	10	yellow
A140	99	28	grey
B125	23	6	brown-yellow
B130	35	12	yellow
B135	63	19	yellow
B140	99	41	grey
C125	44	12	yellow
C130	52	14	grey-yellow
C135	86	23	grey-yellow
C140	100	28	grey

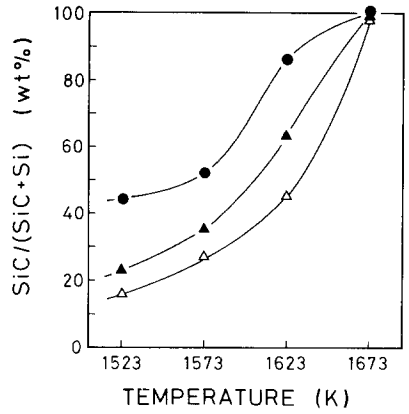

Figure 2 Effect of reaction temperature on carburization ratio, SiC/(SiC + Si). (●) $[SiH_4] = 2.0\,mol\,\%$, FR = $2.7 \times 10^{-5}\,m^3\,sec^{-1}$, (▲) $[SiH_4] = 3.6\,mol\,\%$, FR = $2.7 \times 10^{-5}\,m^3\,sec^{-1}$, (△) $[SiH_4] = 3.6\,mol\,\%$, FR = $1.8 \times 10^{-5}\,m^3\,sec^{-1}$.

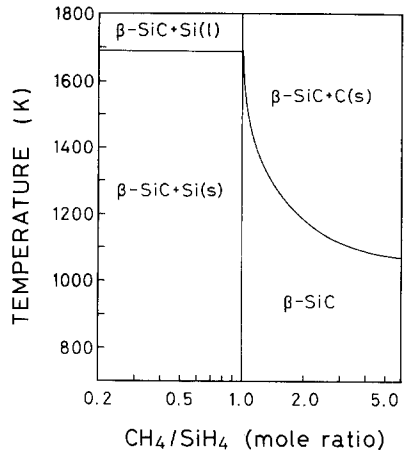

Figure 3 Calculated CVD phase diagram at $[SiH_4 + CH_4] = 6\,mol\,\%$ and $P_{tot} = 0.1\,MPa$.

diffraction pattern, respectively, of the particles obtained at 1623 K. The diffraction pattern indicated that the particles are a composite of polycrystalline β-SiC and silicon. The particles obtained below 1623 K consisted of a silicon core and a β-SiC shell.

The effect of the reaction temperature on the powder density is shown in Fig. 6. The calculated density based on the powder composition using the theoretical densities of β-SiC ($3.21 \times 10^3\,kg\,m^{-3}$) and silicon ($2.33 \times 10^3\,kg\,m^{-3}$) are indicated by broken-lines. The measured densities are consistently smaller than the calculated values. This difference increases with increase of the reaction temperature and total gas flow rate and with a decrease of the reactant concentration. The presence of hollows in the particles leads to this difference.

A typical variation of the particle diameters, d, measured by TEM and the BET equivalent diameters calculated from the specific surface areas with reaction temperature is shown in Fig. 7. Under all experimental conditions the resulting powder showed a smaller value for d_{BET} than for d_{TEM}, and the difference between these values increased with the increase of reaction temperature. The increase of the hollow size may have contributed to this difference. For a fixed gas flow rate, the d_{TEM} decreased with decrease of SiH_4 concentration because at a lower SiH_4 concentration the growth of microcrystallites becomes difficult. At a fixed concentration, the d_{TEM} decreased with increasing gas flow rate. At large gas flow rates the residence time of silicon particles in the furnace is short, thus, the silicon particles become less likely to grow.

Fig. 8 shows the relation between the thicknesses, δ, of the β-SiC shell (δ_{SiC}) as well as the silicon core (δ_{Si}) of the particles and the carburization ratio. The average thicknesses of the β-SiC shell and the silicon core can be calculated using the measured powder density (ϱ) according to Equations 1 and 2, respectively

$$\delta_{SiC} = \frac{d}{2}\left[1 - \left(1 - \frac{x\varrho}{\varrho_{SiC}}\right)^{1/3}\right] \quad (1)$$

$$\delta_{Si} = \frac{d}{2}\left\{\left(1 - \frac{x\varrho}{\varrho_{SiC}}\right)^{1/3} - \left[1 - \frac{x\varrho}{\varrho_{SiC}} - (1 - x)\frac{\varrho}{\varrho_{Si}}\right]^{1/3}\right\} \quad (2)$$

where d is the mean particle diameter and x is the carburization ratio. The subscripts denote the values of the corresponding phases.

The thicknesses of the β-SiC shell and the silicon core can also be calculated from Equations 3 and 4, respectively. These equations apply for the case when β-SiC forms via the diffusion of silicon from the silicon core through the β-SiC shell [7].

TABLE III Specific surface area, BET equivalent diameter, TEM particle size, X-ray mean crystallite size and density of powders

Run no.	Specific surface area ($m^2\,g^{-1}$)	BET equivalent diameter (nm)	TEM mean particle size (nm)	X-ray mean crystallite size (nm)	Powder density ($10^3\,kg\,m^{-3}$)
A125	–	–	–	2.6	2.32
A130	40	60	64 ± 20	2.7	2.44
A135	32	70	80 ± 20	3.4	2.30
A140	72	26	114 ± 22	5.4	2.10
B125	35	69	70 ± 9	3.4	2.43
B130	38	61	64 ± 15	4.0	2.48
B135	35	61	64 ± 15	5.0	2.15
B140	39	48	79 ± 20	5.4	1.90
C125	58	39	46 ± 5	4.4	2.22
C130	42	52	54 ± 10	4.6	2.17
C135	38	51	68 ± 10	5.1	1.92
C140	63	30	73 ± 10	5.6	1.89

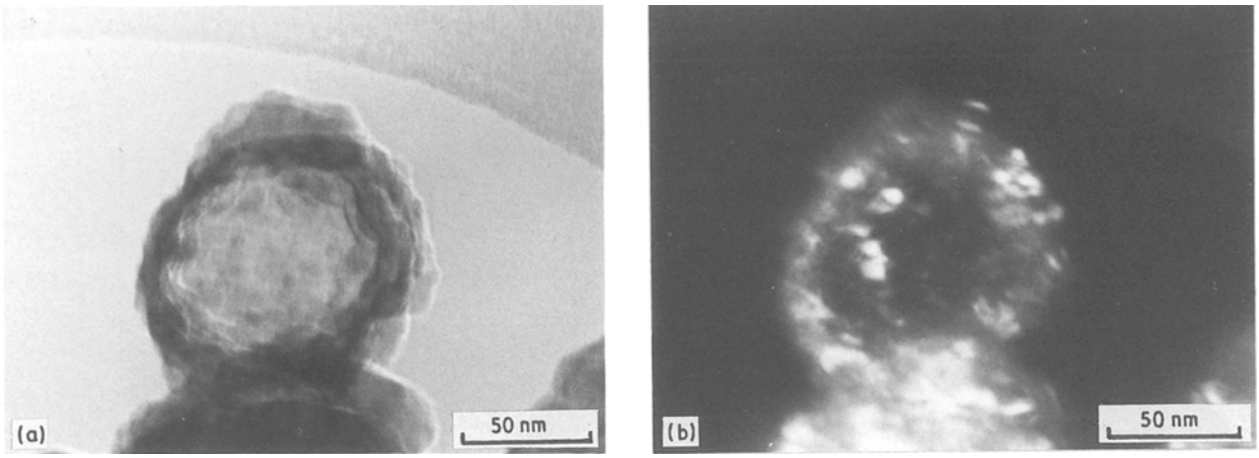

Figure 4 Electron micrographs of the powder prepared at 1673 K, $[SiH_4]$ = 3.6 mol % and FR = 1.8×10^{-5} m^3 sec^{-1}. (a) Bright-field image, (b) β-SiC (1 1 1) dark-field image, (c) electron diffraction pattern.

$$\delta'_{SiC} = \frac{d}{2}\left[1 - \left(1 + \frac{xM_{SiC}}{M_{SiC} - xM_C}\frac{\varrho_{Si}}{\varrho_{SiC}}\right)^{-1/3}\right] \quad (3)$$

$$\delta'_{Si} = \frac{d}{2}\left(1 + \frac{xM_{SiC}}{M_{SiC} - xM_C}\frac{\varrho_{Si}}{\varrho_{SiC}}\right)^{-1/3} \times \left[1 - \left(\frac{xM_{Si}}{M_{SiC} - xM_C}\right)^{1/3}\right] \quad (4)$$

where M is the mole weight. The results calculated from the two methods agreed well, as shown in Fig. 8. This shows that the SiC particles formed through the two-step process mentioned above. The thickness of the β-SiC shell increased from 2 to 10 nm while the thickness of the silicon core decreased from 8 to 0 nm as the carburization ratio increased from 40 to 100 wt %. The thickness of the β-SiC shell are greater than that of the silicon core over the carburization ratio of about 70 wt %. The thicknesses of the β-SiC shell observed by TEM are almost in agreement with the calculated values shown in Fig. 8. Table III summarized the specific surface areas, particle sizes, crystallite sizes and densities of the powders prepared in the present experiment.

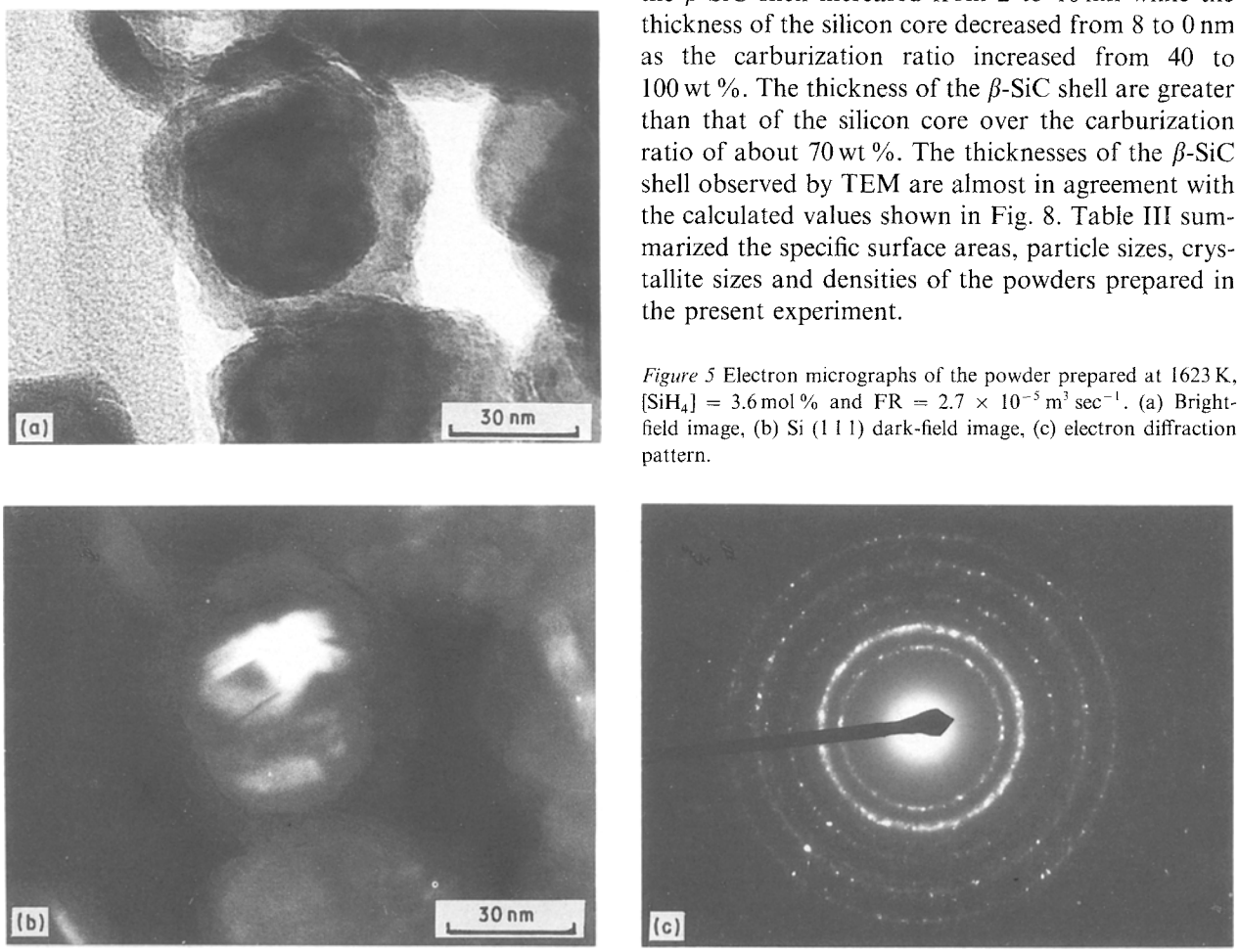

Figure 5 Electron micrographs of the powder prepared at 1623 K, $[SiH_4]$ = 3.6 mol % and FR = 2.7×10^{-5} m^3 sec^{-1}. (a) Bright-field image, (b) Si (1 1 1) dark-field image, (c) electron diffraction pattern.

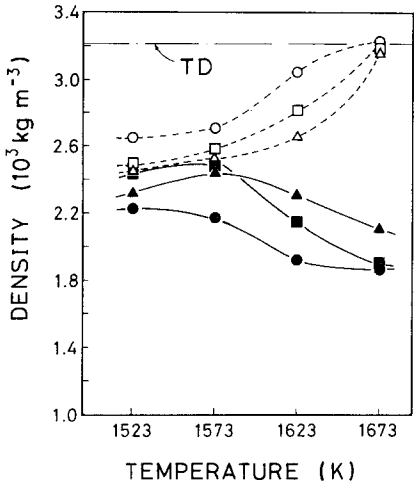

Figure 6 Effect of reaction temperature on powder density. (●, ○) $[SiH_4]$ = 2.0 mol %, FR = 2.7 × 10^{-5} m^3 sec^{-1}, (■, □) $[SiH_4]$ = 3.6 mol %, FR = 2.7 × 10^{-5} m^3 sec^{-1}, (▲, △) $[SiH_4]$ = 3.6 mol %, FR = 1.8 × 10^{-5} m^3 sec^{-1}. TD = theoretical density of β-SiC (3.21 × 10^3 kg m^{-3}). (——) Experimental, (– – –) calculated.

3.3. Infrared absorption

Fig. 9 shows typical IR absorption spectra of powders obtained at FR = 2.7 × 10^{-5} m^3 sec^{-1} and $[SiH_4]$ = 3.6 mol % in the wavenumber range from 400 to 1400 cm^{-1}. Only one absorption peak at about 874 cm^{-1} is predicted for solid (not hollow) spherical β-SiC particles based on the calculation from the surface phonon mode [8]. However, in the present experiment, absorption peaks at 940 and 810 cm^{-1} were observed for the powders prepared below 1623 K. These particles consisted of a β-SiC shell and a silicon core. As the reaction temperature increased, the intensity of the peak at about 940 cm^{-1} decreased and the two peaks shifted so as to approach each other. These splits of the IR absorption peak of the β-SiC particles are considered to be caused by the shape anisotropy of the surface phonon mode due to the extremely thin β-SiC layer of magnitude 2 to 10 nm [9]. For the hollow β-SiC particles obtained at 1673 K, one absorption peak at about 830 cm^{-1} and a shoulder at about 930 cm^{-1} were observed. The IR absorption characteristics from the surface phonon mode of β-SiC particles are described in detail elsewhere [10].

3.4. Lattice parameter of β-SiC

Fig. 10 shows the effect of reaction temperature on the lattice parameter (a) of β-SiC in the powders. The lattice parameter decreases with the increase of both reaction temperature and gas flow rate while at a constant reactant concentration, and also decreases with the decrease of reactant concentration at a constant gas flow rate. Fig. 11 represents the relationship between the lattice parameter and the carburization ratio. The lattice parameter is larger than that of bulk β-SiC crystal (a = 0.435 89 nm) [11] up to the carburization ratio of 70 wt % and decreases with increasing carburization ratio. Beyond the carburization ratio of 70 wt %, the lattice parameter became constant taking the value equivalent to that of bulk β-SiC crystal.

Hase and Suzuki [12] prepared β-SiC powders by solid-phase reactions of C + SiO, C + SiO_2 and

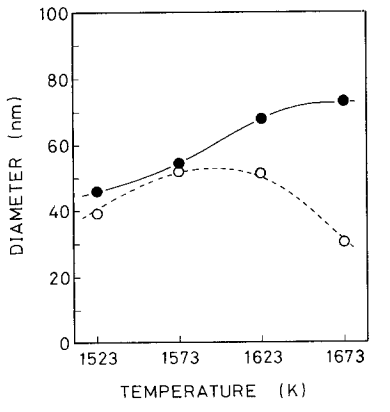

Figure 7 Effect of reaction temperature on particle size. $[SiH_4]$ = 2.0 mol %, FR = 2.7 × 10^{-5} m^3 sec^{-1}. (●) d_{TEM}, (○) d_{BET}.

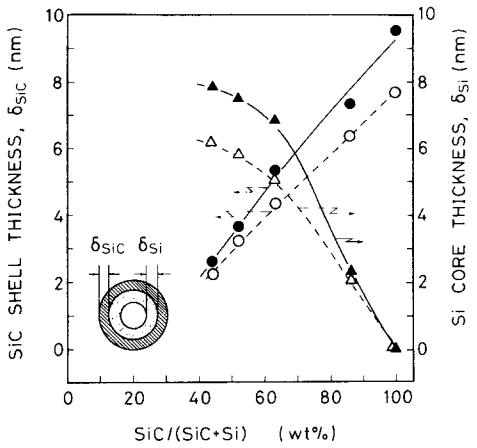

Figure 8 Relationship between the SiC shell thickness as well as the silicon core thickness and carburization ratio (SiC/(SiC + Si)) for the powders prepared at $[SiH_4]$ = 2.0 mol % and FR = 2.7 × 10^{-5} m^3 sec^{-1}. (●) From Equation 1, (▲) from Equation 2, (○) from Equation 3, (△) from Equation 4.

Hase and Suzuki [12] prepared β-SiC powders by solid-phase reactions of C + SiO, C + SiO_2 and

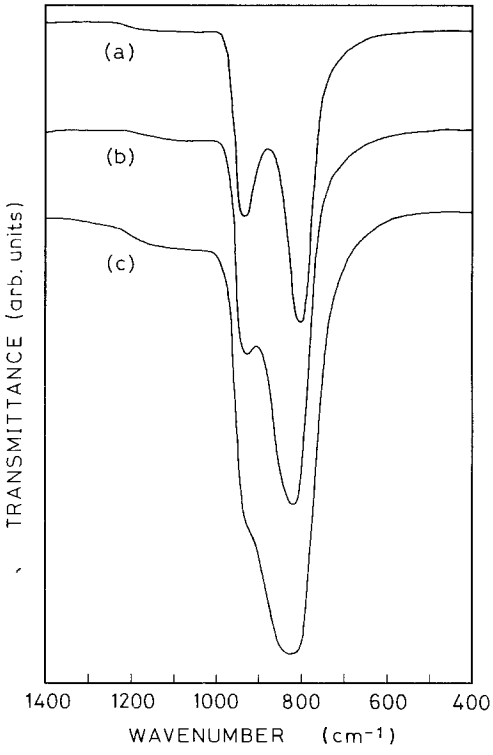

Figure 9 Infrared absorption spectra of the powders prepared at $[SiH_4]$ = 3.6 mol % and FR = 2.7 × 10^{-5} m^3 sec^{-1}. Reaction temperature: (a) 1573 K, (b) 1623 K, (c) 1673 K.

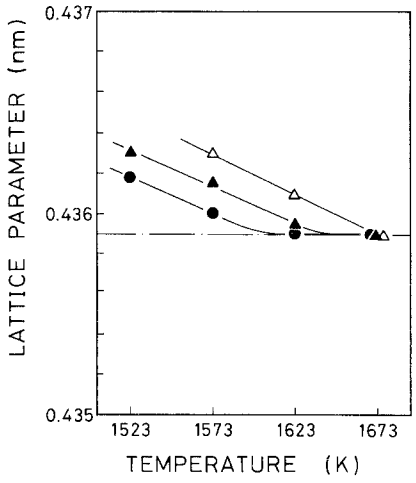

Figure 10 Effect of reaction temperature on the lattice parameter of β-SiC. (●) $[SiH_4]$ = 2.0 mol %, FR = 2.7 × 10^{-5} m^3 sec^{-1}, (▲) $[SiH_4]$ = 3.6 mol %, FR = 2.7 × 10^{-5} m^3 sec^{-1}, (△) $[SiH_4]$ = 3.6 mol %, FR = 1.8 × 10^{-5} m^3 sec^{-1}. (—·—) The value of bulk β-SiC [11].

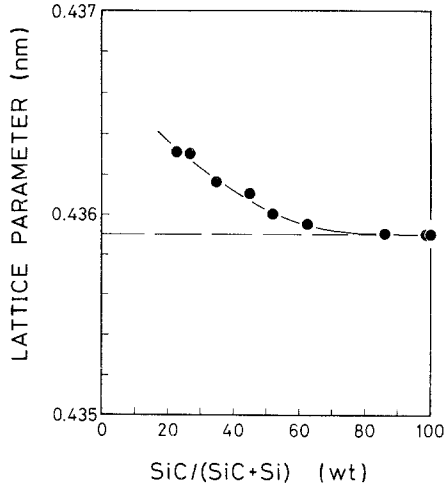

Figure 11 Relationship between the lattice parameter of β-SiC and carburization ratio (SiC/(SiC + Si)). (—·—) The value of bulk β-SiC [11].

C + Si and reported that the lattice parameter of the β-SiC particles containing free carbon was smaller than that of bulk β-SiC crystal. Bonnke and Fitzer [13] prepared β-SiC films containing free carbon by thermal decomposition of $(CH_3)_3SiCl$, $(CH_3)_2SiCl_2$ and CH_3SiCl_3 in H_2. They reported that the lattice parameter decreased as the amount of free carbon increased from 0 to 10 wt %. In these cases, the substitution of silicon atoms having a larger covalent radius (0.117 nm) [14] for carbon atoms having a smaller radius (0.077 nm) [14] is considered to cause the decrease of the lattice parameter of β-SiC. Kawashima and Setaka [15] reported that the lattice parameter of β-SiC films containing free silicon prepared by CVD using $SiCl_4$ and toluene had the same value as that of β-SiC not containing free silicon. Chin *et al.* [16] also reported that the lattice parameter of β-SiC films containing 3 to 50 wt % free silicon prepared by CVD using CH_3SiCl_3 and H_2 was constant, having a value equal to that of a single-phase β-SiC. These results suggest that silicon sites in the β-SiC lattice are substitutionally occupied by carbon atoms, thus resulting in a decrease of lattice parameter, but carbon sites could not be replaced by silicon atoms. Therefore, no change in the value of lattice parameter takes place. On the other hand, it was reported that the lattice structure of β-SiC films deposited on the silicon wafer is remarkably disordered at the SiC/Si interface due to the large lattice mismatch between silicon (a = 0.543 088 nm) [17] and β-SiC (a = 0.435 89 nm) [18, 19]. Consequently when an extremely thin β-SiC layer forms on the silicon body, a lattice mismatch between silicon and β-SiC may take place causing enlargement of the β-SiC lattice parameter. The effect of the lattice mismatch may be greater as the β-SiC shell becomes thinner. When the carburization ratio is more than 70 wt %, the lattice parameter agrees with that of the bulk β-SiC crystal. These results may correspond to the fact that the β-SiC shell becomes thicker than the silicon core at the carburization ratio of greater than 70 wt %, as shown in Fig. 8, thus, reducing the effect of lattice mismatch.

4. Conclusion

Silicon carbide powders (β form) were prepared by CVD of SiH_4–CH_4–H_2 system in the temperature range 1523 to 1673 K. The structure and properties of the resulting powders were investigated. The following results were obtained.

1. The powders of single-phase β-SiC were obtained at 1673 K, while the powders obtained below 1623 K were a composite of silicon and β-SiC. The carburization ratio (SiC/(SiC + Si)) increased with increasing reaction temperature and total gas flow rate, and also increased with decreasing reactant concentration.
2. The TEM average particle sizes increased from 46 to 114 nm with increasing reaction temperature and reactant concentration and increased with decreasing gas flow rate.
3. The particles obtained below 1623 K consisted of a silicon core and β-SiC shell, while those obtained at 1673 K were hollow β-SiC particles.
4. IR absorption peaks were observed at 810 and 940 cm^{-1} for the particles consisting of a silicon core and a β-SiC shell. The hollow β-SiC particles exhibited an IR peak at about 830 cm^{-1} and a shoulder at about 930 cm^{-1}.
5. When the carburization ratio was less than 70 wt %, the lattice parameter of β-SiC was larger than that of the bulk β-SiC crystal. As the carburization ratio increased, the lattice parameter of β-SiC decreased until it equalled that of bulk β-SiC crystal, and became constant as the carburization ratio exceeded 70 wt %.

Acknowledgements

The authors thank Messrs T. Sekiguchi and H. Ohta for TEM observations, Mr F. Chida for measurements of IR absorption spectra and Professor R. Watanabe for helpful discussions. This research was supported in part by the Grand-in-Aid for Scientific Research from the Ministry of Education, Science and Culture under Contract Nos. 60 430 019 and 60 850 130.

References

1. K. NIIHARA, T. YAMAMOTO, J. ARIMA, R. TAKEMOTO, K. SUGANUMA, R. WATANABE, T. NISH-

IKAWA and M. OKUMURA, in "Ultrastructure Processing of Advanced Ceramics", edited by J. D. Mackenzie and D. R. Ulrich (Wiley, New York, 1988) p. 547.
2. K. KOUMOTO, M. SHIMOHIGOSHI, S. TAKEDA and H. YANAGIDA, *J. Mater. Sci. Lett.* **6** (1987) 1453.
3. T. HIRAI and T. GOTO, in "Tailoring Multiphase and Composite Ceramics", Materials Science Research, Vol. 20, edited by R. E. Tressler, G. L. Messing, C. G. Pantano, R. E. Newnham (Plenum, New York, 1986) p. 165.
4. T. HIRAI, M. SASAKI and M. NIINO, *J. Soc. Mater. Sci. Jpn.* **36** (1987) 1205.
5. T. GOTO and T. HIRAI, *Nippon Kagaku Kaishi* **11** (1987) 1939.
6. Y. OKABE, J. HOJO and A. KATO, *ibid.* **2** (1980) 188.
7. A. KATO, J. HOJO and Y. OKABE, *Mem. Fac. Engng Kyushu Univ.* **41** (1981) 319.
8. L. D. CHEN, T. GOTO and T. HIRAI, in Proceedings of Sintering '87, Tokyo, edited by S. Somiya, M. Shimada, M. Yoshimura and R. Watanabe (Elsevier, London, 1988) p. 49.
9. L. D. CHEN, T. GOTO and T. HIRAI, in Abstracts of the 26th Symposium on Basic Science of Ceramics, Nagoya, Japan, January 20–22 (1988) 114.
10. L. D. CHEN, T. GOTO and T. HIRAI, *J. Mater. Sci.* to be published.
11. "Powder Diffraction File", JCPDS International Centre for Diffraction Data, (1979) File No. 29-1129.
12. T. HASE and H. SUZUKI, *Yogyo-Kyokai-Shi* **86** (1978) 541.
13. VON M. BONNKE and E. FITZER, *Ber. Dtsch. Keram. Ges.* **43** (1966) 180.
14. L. PAULING, in "The Nature of the Chemical Bond" (Cornell University Press, Ithaca, New York, 1960) p. 225.
15. C. KAWASHIMA and N. SETAKA, *Yogyo-Kyokai-Shi* **75** (1967) 74.
16. J. CHIN, P. K. GANTZEL and R. G. HUDSON, *Thin Solid Films* **40** (1977) 57.
17. "Powder Diffraction File", JCPDS International Centre for Diffraction Data, (1977) File No. 27-1402.
18. I. H. KHAN, *Mater. Res. Bull.* **4** (1969) 285.
19. K. KUROIWA and T. SUGANO, *J. Electrochem. Soc.* **120** (1973) 138.

Received 27 June
and accepted 8 December 1988